Kondo effect at low electron density and high particle-hole asymmetry in 1D, 2D, and 3D

Rok Žitko[1,2] and Alen Horvat[1]
[1]*Jožef Stefan Institute, Jamova 39, SI-1000 Ljubljana, Slovenia*
[2]*Faculty of Mathematics and Physics, University of Ljubljana, Jadranska 19, SI-1000 Ljubljana, Slovenia*
(Received 8 July 2016; revised manuscript received 6 September 2016; published 21 September 2016)

Using the perturbative scaling equations and the numerical renormalization group, we study the characteristic energy scales in the Kondo impurity problem as a function of the exchange coupling constant J and the conduction-band electron density. We discuss the relation between the energy gain (impurity binding energy) ΔE and the Kondo temperature T_K. We find that the two are proportional only for large values of J, whereas in the weak-coupling limit the energy gain is quadratic in J, while the Kondo temperature is exponentially small. The exact relation between the two quantities depends on the detailed form of the density of states of the band. In the limit of low electron density the Kondo screening is affected by the strong particle-hole asymmetry due to the presence of the band-edge van Hove singularities. We consider the cases of one- (1D), two- (2D), and three-dimensional (3D) tight-binding lattices (linear chain, square lattice, cubic lattice) with inverse-square-root, step-function, and square-root onsets of the density of states that are characteristic of the respective dimensionalities. We always find two different regimes depending on whether T_K is higher or lower than μ, the chemical potential measured from the bottom of the band. For 2D and 3D, we find a sigmoidal crossover between the large-J and small-J asymptotics in ΔE and a clear separation between ΔE and T_K for $T_K < \mu$. For 1D, there is, in addition, a sizable intermediate-J regime where the Kondo temperature is quadratic in J due to the diverging density of states at the band edge. Furthermore, we find that in 1D the particle-hole asymmetry leads to a large decrease of T_K compared to the standard result obtained by approximating the density of states to be constant (flat-band approximation), while in 3D the opposite is the case; this is due to the nontrivial interplay of the exchange and potential scattering renormalization in the presence of particle-hole asymmetry. The 2D square-lattice density of states behaves to a very good approximation as a band with constant density of states.

DOI: 10.1103/PhysRevB.94.125138

I. INTRODUCTION

In experimental setups designed for studying the Kondo effect in quantum dots and other nanostructures, the leads attached to the device are typically low-dimensional electron systems such as a two-dimensional electron gas or even an effectively one-dimensional nanowire. Since the electron density in such systems is tunable, it may occur that at low enough electron density the chemical potential lies close to the band-edge singularities in the density of states (DOS) of the reservoir. In such a situation there is an extreme asymmetry between the particle and hole states [1]. This affects the Kondo screening of the local moment and leads to significant deviations from the standard results obtained in the flat-band approximation that assumes a featureless (i.e., constant) DOS [2].

This work explores the Kondo physics at low electron density n so that the chemical potential μ is close to the bottom of the band. We discuss three paradigmatic types of band-edge van Hove singularities: the inverse-square-root divergency at the bottom of the one-dimensional (1D) DOS, the step-function singularity in the two-dimensional (2D) DOS, and the square-root onset in the three-dimensional (3D) DOS. These energy dependencies are directly dictated by the dimensionality of the system and always occur [assuming that the dispersion relation $\epsilon(k)$ is differentiable close to its global minimum in the Brillouin zone, which is generally the case]. To be specific, we use the 1D tight-binding chain DOS, the 2D square-lattice DOS, and the 3D cubic-lattice DOS, while the magnetic impurity is described using the spin-1/2 Kondo model. The problem is studied using the numerical renormalization group (NRG) [3–5] with a discretization technique that is applicable to arbitrary DOS without any systematic discretization errors [6,7]. We compare numerical results to the predictions from the perturbative renormalization-group arguments [1]. We pay particular attention to the different behaviors of the energy gain due to the impurity ΔE and the Kondo temperature T_K. ΔE is calculated by subtracting the ground-state energy of the system with and without the impurity,

$$\Delta E = E_0(0) - E_0(J). \tag{1}$$

This is hence the energy required to remove the impurity from the system (i.e., an impurity binding energy). T_K is determined as the temperature at which the effective impurity moment is reduced to small numbers, defined according to Wilson as [3,4]

$$T_K \chi_{\rm imp}(T_K) = 0.07, \tag{2}$$

where $\chi_{\rm imp}$ is the impurity contribution to the magnetic susceptibility,

$$\chi_{\rm imp} = \langle S_z^2 \rangle_J - \langle S_z^2 \rangle_0, \tag{3}$$

and 0.07 is some essentially arbitrary small number. It will be seen that ΔE and T_K are, in general, not proportional to each other and have different asymptotic behaviors in the weak-coupling limit. We also present a scaling argument that explains the reduction of T_K in 1D and its enhancement in 3D for small density: they are due to the *curvature* in the DOS close to band edges. In the appendixes we consider the effect of

the magnetic field and of the anisotropy in the Kondo coupling. We also calculate analytically the quadratic energy gain due to a magnetic impurity in the $J \to 0$ limit in the flat-band approximation.

II. MODEL

We consider the Kondo impurity model

$$H = J\mathbf{s}\cdot\mathbf{S} + \sum_{\mathbf{k}a} \epsilon_{\mathbf{k}} c^\dagger_{\mathbf{k}a} c_{\mathbf{k}a}, \tag{4}$$

where J is the Kondo exchange coupling constant;

$$\mathbf{s} = \frac{1}{2}\sum_{ab} f^\dagger_a \boldsymbol{\sigma}_{ab} f_b \tag{5}$$

is the local spin density at the position of the impurity, with $a,b \in \{\uparrow,\downarrow\}$ and the local operator at the origin f defined as

$$f^\dagger_a = \frac{1}{\sqrt{N}}\sum_{\mathbf{k}} c^\dagger_{ka}, \tag{6}$$

with N being the number of sites forming the lattice; $\mathbf{S}$ is the impurity spin-1/2 operator,

$$\mathbf{S} = \tfrac{1}{2}\boldsymbol{\sigma}; \tag{7}$$

and the conduction-band part of the Hamiltonian corresponds to either a 1D chain, a 2D square-lattice, or a 3D cubic-lattice tight-binding model. The only information about the conduction band that is relevant for the impurity model is its density of states $\rho(\epsilon)$, which is known in analytical form for all three dimensions. The chemical potential is measured from the bottom of the band; thus $\mu = 0$ corresponds to a completely depleted band.

The calculations are done within the grand-canonical ensemble in the true thermodynamic limit; thus both the system size and the total number of electrons are infinite: the band filling n is controlled by μ, while $L,N \to \infty$. The NRG discretization is performed using the method described in Ref. [6], which correctly handles arbitrary DOS even in the presence of singularities [8]. This approach allows us to calculate the energy gain ΔE to extremely high accuracy [9] by performing two NRG runs, one for a finite J and another for a reference system with decoupled impurity ($J = 0$), then subtracting the obtained ground-state energies of the discrete Wilson-chain representations; while these two energies depend significantly on the details of the NRG discretization, their difference does not and, in fact, changes very little with varying the value of the discretization parameter Λ if the appropriate discretization scheme is used [9]. The numerical calculations are performed for $N_z = 8$ twisted discretization grids and with the discretization parameter $\Lambda = 2$ [3,6]. The truncation cutoffs are taken high enough so that the results are fully converged. The temperature is effectively zero. The results will be presented in units of half bandwidth $D = 2dt$, where d is the dimensionality of the tight-binding lattice.

III. CHARACTERISTIC ENERGY SCALES

A. Binding energy ΔE

We first discuss the relevant parameter regimes of the exchange coupling J. We find that in all cases, irrespective of the energy dependence of the DOS and the nature of the singularities, the small-J and large-J regimes behave exactly the same (see Fig. 1).

In the large-J regime, we find the expected result that the energy gain is $\Delta E = 3J/4$ due to the formation of a local singlet state between the impurity spin and the lattice site to which the impurity is attached. This regime is reached for $J \gg D$. In all cases considered, the numerical value of ΔE lies atop the $3J/4$ line within the accuracy of linewidth for $J/D \gtrsim 10$.

In the small-J regime we find quadratic behavior with a nonuniversal prefactor α that depends on the DOS ($d = 1,2,3$) and the band occupancy n,

$$\Delta E = \alpha_d(n) J^2. \tag{8}$$

It should be emphasized that ΔE is not of the order of T_K for small J, as often claimed. The difference is perhaps underappreciated because the common intuition is that the energy gain in the formation of the Kondo singlet state should be approximately T_K since the singlet forms on that energy scale. In fact, the situation is somewhat more subtle because of the logarithmic scaling of the exchange coupling in the Kondo mechanism [2,10]. Many decades of bulk excitations above T_K (in the scaling regime $T_K \ll \epsilon \ll J$) are already slightly perturbed by the exchange scattering off the magnetic

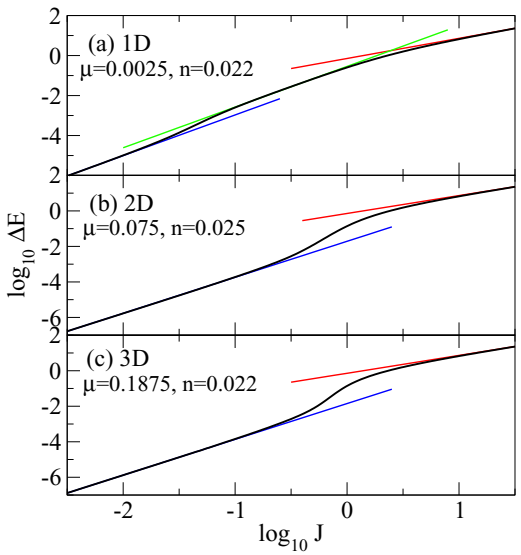

FIG. 1. Overview of the different parameter regimes in the 1D, 2D, and 3D cases. The energy gain ΔE is plotted as a function of the Kondo exchange coupling J on a log-log scale. The red and blue lines are the high-J and low-J asymptotics, $\propto J$ and $\propto J^2$, respectively, common for all three dimensions. For the 1D case in (a) we also indicate the intermediate-J regime, which is $\propto J^2$ (green line). The model parameters are indicated in the respective panels. They are chosen so that the band occupancy is comparable in all three cases, $n \approx 0.02$.

impurity. The degree of perturbation can be quantified through the quasiparticle phase shift of the bath electron with energy ϵ, $\delta(\epsilon)$. The phase shift for $\epsilon \gg J$ is essentially zero because in this range the bath electron spin is hardly affected by the impurity. The local moment starts to be felt on the energy scale $\epsilon \sim J$, but the effect is weak, and the phase shift is $\sim J/D$. At still lower energies, the phase shift then increases logarithmically, until for ϵ on the scale of T_K it reaches saturated values of the order of 1 [recall that $\delta(\epsilon = 0) = \pi/2$ for the Kondo effect at the particle-hole-symmetric point]. The total energy gain is given as an integral of the single-particle energy shifts approximately proportional to $\delta(\epsilon)$ over all energies ϵ, and since the contribution is $\sim J$ for all $\epsilon \lesssim J$, we expect the result to scale as $\Delta E \propto J^2$. The behavior $\Delta E \propto J^2$ is indeed seen in the numerical calculations of this quantity using the NRG in all models of this class. Since the Kondo problem is known to be nonperturbative in J, the actual expression must, in fact, be of the form $\Delta E = f(J) + g(J)$, where $f(J)$ is an analytical function which is quadratic in the $J \to 0$ limit, while $g(J)$ is a nonanalytical exponentially small correction which may be neglected in the $J \to 0$ limit compared to the first term. The leading correction due to dynamical processes in $f(J)$ is actually $O(J^3)$ and hence analytical (see Appendix B).

Another quantity of interest is the expectation value of $\langle \mathbf{S} \cdot \mathbf{s} \rangle$, i.e., of the interaction term in the Kondo Hamiltonian. Since this term is coupled linearly to J, it can be estimated through $d\langle H \rangle / dJ = -d\Delta E/dJ$. Since $\langle \mathbf{S} \cdot \mathbf{s} \rangle \propto J$ [see Figs. 2(a) and 2(b)], by integration of ΔE over J we again find $\Delta E \propto J^2$. In fact, it is interesting to compare ΔE with the quantity

$$(\Delta E)_{\rm int} = J|\langle \mathbf{S} \cdot \mathbf{s} \rangle| \tag{9}$$

[see Fig. 2(c)]. As expected, in the large-J limit the full contribution to the energy gain comes from the singlet localized at the position of the impurity. The low-J limit of the ratio $(\Delta E)_{\rm int}/\Delta E$ is exactly 2; this is found universally for all values of filling and for all three dimensionalities. In fact, this follows directly from the quadratic behavior of ΔE. Namely,

$$\frac{(\Delta E)_{\rm int}}{\Delta E} = \frac{J(d\Delta E/dJ)}{\Delta E} = \frac{d\ln \Delta E}{d\ln J}; \tag{10}$$

thus the plot in Fig. 2(c) actually represents the logarithmic derivative of ΔE from which we can directly read off the local power-law exponent β at given J. It then follows that

$$\begin{aligned} (\Delta E)_{\rm int} &= \beta \Delta E, \\ (\Delta E)_{\rm kin} &= (1-\beta)\Delta E, \end{aligned} \tag{11}$$

where the kinetic part $(\Delta E)_{\rm kin} = (\Delta E) - (\Delta E)_{\rm int}$. This result indicates that asymptotically, for $J \to 0$, twice the binding energy is always contributed by the local $\mathbf{s}(\mathbf{r} = 0)$ term, while the kinetic part $(\Delta E)_{\rm kin}$ is actually negative and equal in absolute value to ΔE. In the high-J limit, we have $\beta = 1$; thus the energy gain is entirely due to the local interaction term with no correction from the bulk. Figure 2(c) also indicates that $\beta > 1$ at any finite J; thus the binding (energy gain) is always due to the interaction term, while the kinetic term always reduces the binding since it is strictly negative.

Returning now to the discussion of the different regimes of J in relation to Fig. 1, we note a clear difference between the 2D and 3D cases and the 1D case. In 2D and 3D, the low-J and high-J asymptotic regimes of ΔE are connected by a single sigmoidal crossover curve whose inflection point is slightly below $J = 1$, and the low-J asymptotic regime is reached at $J \approx 0.2$. In 1D, the behavior is qualitatively different: at $J \approx 3$ we observe a very smooth crossover from the $3J/4$ behavior to an intermediate J^2 regime which extends to very low J values; then at $J \approx 0.03$ there is a crossover to the asymptotic weak-coupling J^2 regime with a different prefactor [see Fig. 1(a)]. This is, in fact, the physics discussed in Ref. [1]: when the characteristic energy scale, such as ΔE or T_K, is larger than μ, the system is sensitive to the diverging DOS at the bottom of the conduction band in one dimension, and the system is in a different universality class, namely, the class associated with the density of states that diverges as a power law at the Fermi level [11]. When the characteristic scale is below μ, however, we recover the more conventional Kondo screening behavior as found in 2D and 3D.

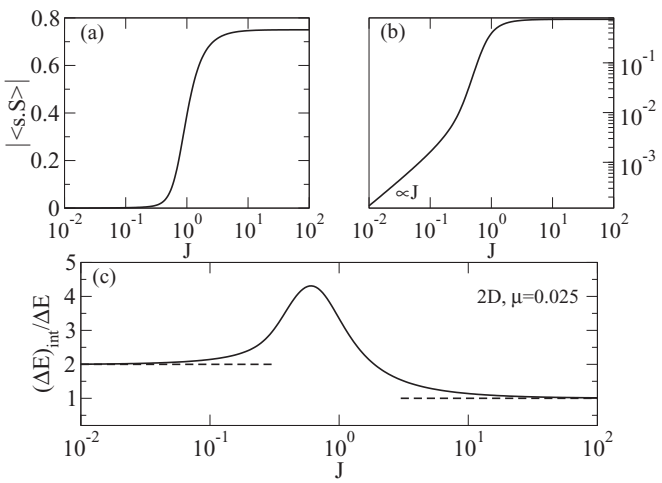

FIG. 2. (a) and (b) Absolute value of the spin-spin expectation value $|\langle \mathbf{s} \cdot \mathbf{S} \rangle|$, i.e., the correlation between the impurity spin and the conduction-band spin at the location of the impurity, plotted on log-linear and log-log scales. (c) Ratio between the local contribution to the energy gain $(\Delta E)_{\rm int} = J|\langle \mathbf{s} \cdot \mathbf{S} \rangle| \propto J^2$ and the total energy gain ΔE. The calculations are performed for 2D DOS with $\mu = 0.025$.

B. Kondo temperature T_K

We now directly compare the energy gain ΔE and the Kondo temperature T_K in Fig. 3. We recall that T_K is defined thermodynamically through the impurity magnetic susceptibility according to Wilson's prescription $T_K \chi_{\rm imp}(T_K) = 0.07$ [3]. This is thus the temperature scale on which the impurity magnetic moment becomes quenched, irrespective of the mechanism of how this actually occurs (via the Kondo effect of conventional or unconventional type or via local singlet formation). We find that the two quantities are proportional in the crossover intermediate-J and large-J regimes, $\Delta E \approx cT_K$, where c is a nonuniversal prefactor of the order of 1. For large J, T_K cannot be directly calculated in the NRG, but our definition through moment quenching is consistent with T_K behaving as $T_K \sim J$ in the large-J limit; thus in this sense the proportionality persists there. For small J, however, T_K

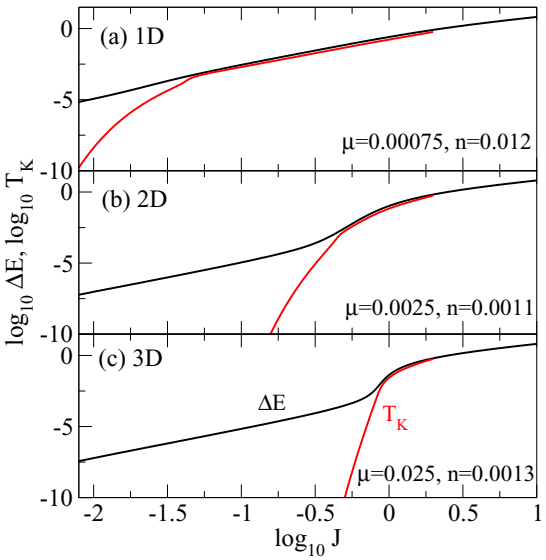

FIG. 3. Relation between the energy gain ΔE and the Kondo temperature T_K for three different dimensionalities. The two quantities behave similarly only in the intermediate-coupling regime but have very different weak-coupling asymptotic behavior.

behaves exponentially,

$$T_K \sim \exp(-1/\rho_0 J), \tag{12}$$

while ΔE is quadratic, as discussed above. [Here $\rho_0 = \rho(\mu)$ is the density of states at the Fermi level, which depends on the value of electron density n.] Indeed, we find that the lower-J boundary of the intermediate-J regime is defined precisely by the point where the two quantities run apart. This is especially pronounced in 1D [1] but also occurs in 2D and 3D.

C. Onset of the Kondo scaling regime

The difference between ΔE and T_K in the weak-coupling limit for $T_K < \mu$ should not be too surprising because the Kondo effect is something which happens in the conduction band due to the presence of the impurity, possibly involving bulk electrons far away from its position, while the impurity binding is more locally sensitive. It is also interesting to compare the temperature dependences of the impurity susceptibility $T\chi_{\rm imp}(T)$ and of the expectation value $\langle \mathbf{s}\cdot\mathbf{S}\rangle(T)$ (see Fig. 4). It is found that the expectation value reaches its saturated value on the scale $T \sim 10^{-2}$, significantly above ΔE. which is here equal to 4×10^{-4}, while the impurity local moment is quenched at much lower temperatures.

If, however, a similar comparison is performed in the parameter range where ΔE and T_K are proportional, i.e., for $T_K > \mu$, we find that both $T\chi_{\rm imp}(T)$ and $\langle \mathbf{s}\cdot\mathbf{S}\rangle(T)$ saturate on the same temperature scale. In addition, we find that $T\chi_{\rm imp}(T)$ does not show universal Kondo behavior at low temperatures in such cases.

From these observations we conclude that the separation between ΔE and T_K is actually a sign of the onset of a true conventional Kondo effect where the spin is quenched through the gradual scaling of the effective exchange coupling J from a small bare value J to the strong-coupling regime, so that the thermodynamic quantities show universal behavior. This

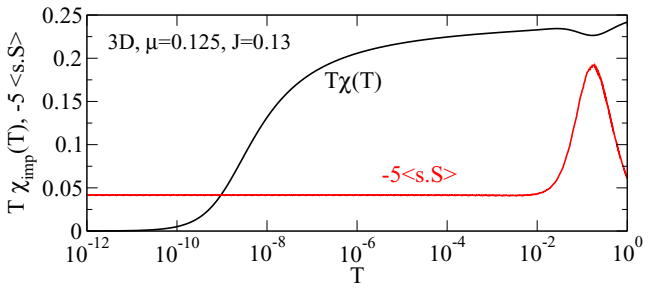

FIG. 4. Temperature dependence of the impurity magnetic susceptibility $T\chi_{\rm imp}(T)$ and of the spin-spin correlation $\langle \mathbf{s}\cdot\mathbf{S}\rangle$ in the parameter regime where ΔE and T_K are already significantly separated.

regime occurs when the Kondo temperature is smaller than the distance of the Fermi level from the band edge, as quantified by μ.

All other cases, where $\Delta E \propto T_K$, are an indication of unconventional local moment quenching mechanisms, either through the trivial local singlet formation for large J or through an unconventional flow of the RG equations due to extreme particle-hole asymmetry due to diverging DOS, as in the 1D case. To conclude, as soon as the physics is appreciably and simultaneously affected by the band on all energy scales, including the states at the very edge of the band, so that the energy scales can no longer be nicely separated into logarithmic chunks, the binding energy ΔE and the local moment quenching scale T_K become equivalent.

IV. KONDO TEMPERATURE AT LOW DENSITY

A. Prefactors

Finally, we discuss the quantitative effects of the band-edge singularities in the DOS on the scaling of the Kondo temperature against J. We plot the logarithm of the Kondo temperature versus $1/\rho_0 J$, where ρ_0 is the density of states at the Fermi level, for a range of n from the half filling, $n = 1/2$, to very small values of the density (see Fig. 5). The nonuniversal behavior for intermediate and large J is due to band-edge singularities and therefore depends on the dimensionality of the system. For small J, however, the exponential behavior $T_K \sim \exp(-1/\rho_0 J)$ is always eventually recovered, and we find straight lines with essentially equal slope. We emphasize that the main effect of the n dependence is already included through the DOS at the Fermi level, $\rho_0 = \rho(\mu)$; thus the trend indicated by the arrows in Fig. 5 (oriented from half filling to small-n range) is due to the differences contained in the prefactor $c_d(\mu)$ to the exponential term in the expression for T_K:

$$T_K = c_d(\mu)\exp[-1/\rho_0 J].$$

Here we find notable differences that can be ascribed solely to the dimensionality-dependent singularities in the DOS: in 1D, the prefactor c_1 at constant $\rho_0 J$ decreases with decreasing filling n, leading to lower T_K, while exactly the opposite behavior is found in the prefactor c_3 for the 3D case. The 2D case is in the intermediate situation with curves that are overlapping to a good approximation; hence c_2 is

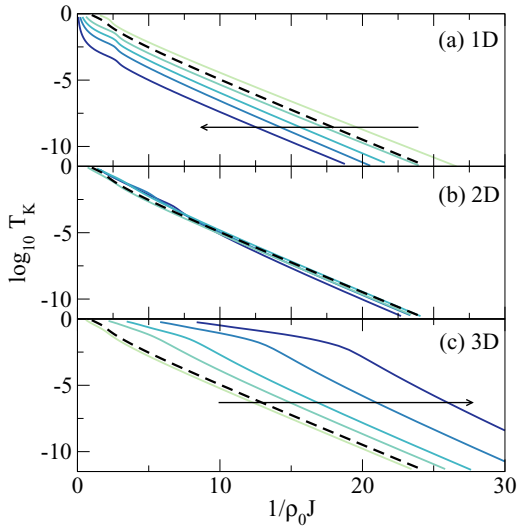

FIG. 5. Asymptotic scaling of the Kondo temperature. We plot the logarithm of T_K versus $1/\rho_0 J$, where ρ_0 is the density of states in the conduction band at the Fermi level, $\rho_0 = \rho(\mu)$. The dashed line indicates the standard result for a flat density of states. The arrows indicate the direction of reduced band filling n, i.e., going toward a more asymmetric situation. In (a) we plot $n = 0.012$, 0.041, 0.074, 0.12, and 0.5, in (b) we plot $n = 0.0011$, 0.0083, 0.085, and 0.39, and in (c) we plot $n = 0.0013$, 0.0032, 0.012, 0.035, and 0.5.

approximately constant. To be more precise, close to the band edge (for μ small compared to the half bandwidth $D = 2dt$), we find that the prefactors $c_d(\mu)$ can be approximated fairly well as

$$\begin{aligned} c_1 &\approx \mu, \\ c_2 &\approx D, \\ c_3 &\approx 25.5 D \exp[-9.5\sqrt{\mu/D}]. \end{aligned} \tag{13}$$

B. Scaling equations for particle-hole-asymmetric band

The differences between the three dimensionalities are too large to be ascribed solely to the effect of the filling dependence of the effective bandwidth. Instead, they must be ascribed to the renormalization of the exchange coupling due to potential scattering, $\rho_0 J \to \rho_0 J_{\text{eff}}$. There is no bare potential term in the Hamiltonian, but it is generated by the renormalization flow when the particle-hole symmetry is broken away from half filling. We now provide an analytical account of this behavior. The scaling equations for the spin-1/2 Kondo model with the Hamiltonian expressed in the form

$$H_{\text{imp}} = J\mathbf{S}\cdot\mathbf{s} + Vn, \tag{14}$$

where V is the potential and $n = \sum_a f_a^\dagger f_a$ is the local density of bulk electrons at the position of the impurity, are [2,12]

$$\begin{aligned} \frac{dJ}{d\ln D} &= -\frac{\rho_+}{2} J^2 + 2\rho_- JV, \\ \frac{dV}{d\ln D} &= \rho_- \left(\frac{3}{16} J^2 + V^2\right), \end{aligned} \tag{15}$$

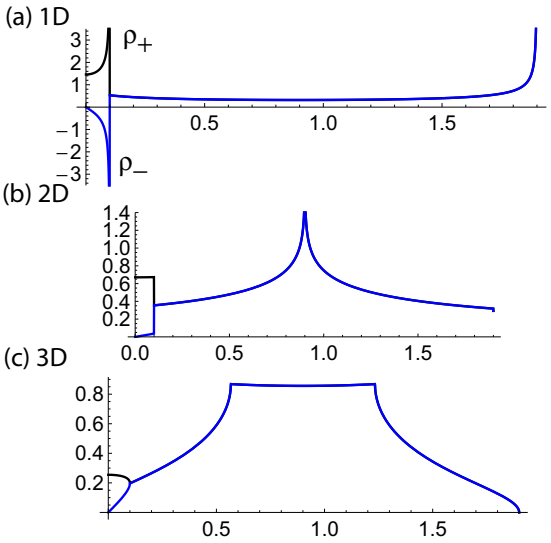

FIG. 6. Symmetric and antisymmetric combinations of the conduction-band density of states that affects the renormalization flow: $\rho_\pm(\epsilon) = \rho(\epsilon) \pm \rho(-\epsilon)$. Here $\mu = 0.1$.

where

$$\begin{aligned} \rho_+ &= \rho(D) + \rho(-D), \\ \rho_- &= \rho(D) - \rho(-D) \end{aligned} \tag{16}$$

are the symmetric and antisymmetric combinations of the density of states in the empty and filled parts of the band, with the energy argument ϵ of $\rho(\epsilon)$ now measured with respect to the Fermi level. These equations are fully general and are valid for arbitrary $\rho(\epsilon)$.

It has been shown that the potential scattering in asymmetric bands with nonzero ρ_- may play an important role [12]. By inspection of the scaling equation for J we see that if V and ρ_- are of the same sign, the growth of J with decreasing bandwidth slows down (T_K is reduced), and the opposite is the case if V and ρ_- are of opposite signs (T_K is increased). The scaling equation for V tells us that if the bare V is zero, effective potential scattering will be generated by the exchange scattering in second order so that V is of the *opposite* sign as ρ_-. Thus an asymmetric DOS might be expected to always lead to a higher Kondo temperature irrespective of the sign of ρ_-.

We now consider our actual problem to see that the situation is slightly more subtle. There are two energy regions. In the high-energy region (i) for $|\epsilon| > \mu$ only the renormalization due to the nonoccupied high-energy states between μ and the upper band edge D contributes. Then $\rho_+(\epsilon) = \rho_-(\epsilon) = \rho(+\epsilon) > 0$ (see Fig. 6). This will generate a potential scattering V with a negative sign. While the detailed form of ρ depends on the dimensionality, the qualitative behavior is the same in all three cases.

In the low-energy region (ii) for $|\epsilon| < \mu$ there will be both particlelike and holelike processes. The behavior of ρ_+ and ρ_- in this region strongly depends on the dimensionality because close to the band edge ρ is concave in 3D, approximately flat in 2D, and convex in 1D. For this reason, in 3D ρ_- is positive, and in 2D ρ_- is approximately zero, while in 1D ρ_- is negative (see Fig. 6); these differences become increasingly pronounced

the closer μ gets to the band edge due to the curvature of the DOS. Thus in 3D $V\rho_- < 0$ and T_K will tend to be increased, as indeed observed in Fig. 5(c) for the increasingly asymmetric band (smaller electron density), as indicated by the arrow. In 1D, however, $V\rho_- > 0$ and T_K will be reduced, again in line with the NRG results in Fig. 5(a). Finally, in 2D with $\rho_- \approx 0$ due to the approximate flatness, the potential scattering term does not play a significant role in the renormalization of J; thus we recover results which nearly overlap with those obtained in the flat-band approximation [see Fig. 5(b)].

The numerical solutions of the scaling equations can indeed be fitted to $T_K = c_d(\mu)\exp(-1/\rho_0 J)$ with $c_d(\mu)$ given by Eqs. (13) with some small deviations due to the scaling equations being truncated at the second order in J and V, while the NRG includes processes to all orders.

V. CONCLUSION

This work explored two issues: (1) the characteristic low-energy scales of the Kondo impurity model, focusing in particular on the difference between the binding energy ΔE and the local moment quenching scale T_K, and (2) the effects due to the band-edge van Hove singularities characteristic of the different dimensionalities of the conduction band, which lead to significant effects in the regime of very low electron density. We showed that in the asymptotic weak-coupling low-J (scaling) regime the binding energy is quadratic in J, while the Kondo temperature is exponentially small. While it is meaningful to compare the scale T_K to other magnetic coupling scales (such as the Ruderman–Kittel–Kasuya–Yosida (RKKY) coupling J_{RKKY}) when discussing the competition between the Kondo screening and magnetic ordering because this decides the fate of the effective moment for temperatures below $\max(T_K, J_{\mathrm{RKKY}})$, this does not imply that an isolated impurity reduces the total ground-state energy only by T_K. Instead, T_K is only a minor correction to the total energy gain arising from the exchange coupling of the impurity with bulk electrons, which is $\propto J^2$. Concerning the dimensionality, we find that the case of 2D is the closest to the conventional Kondo scenario because in the relevant low-energy range the 2D DOS is approximately flat. For low J, the Kondo temperature is thus given by the standard expression $T_K \approx D\exp(-1/\rho_0 J)$. In 1D and 3D we find notable deviation in opposing directions. For the 3D case with concave DOS, the Kondo temperature is increased for reduced band filling: $T_K \approx 25.5D\exp[-9.5\sqrt{\mu/D}]\exp(-1/\rho_0 J)$. For the 1D case, we find that the Kondo temperature in some range of exchange couplings J such that $T_K > \mu$ is a quadratic function of J, while for small J the exponential dependence is recovered. Since the 1D DOS is convex, we find that the Kondo temperature decreases compared to the standard flat-band value for reduced band filling: $T_K \approx \mu\exp(-1/\rho_0 J)$.

Similar trends are expected for other impurity models such as the Anderson impurity model. There the detailed behavior will also depend on the intrinsic potential scattering (bare V after the Schrieffer-Wolff transformation). It should also be noted that in the context of the dynamical mean-field theory the effective impurity model is actually in the intermediate-coupling regime where $\Delta E \propto T_K$; thus the energy gain and the coherence temperature are expected to be of the same scale.

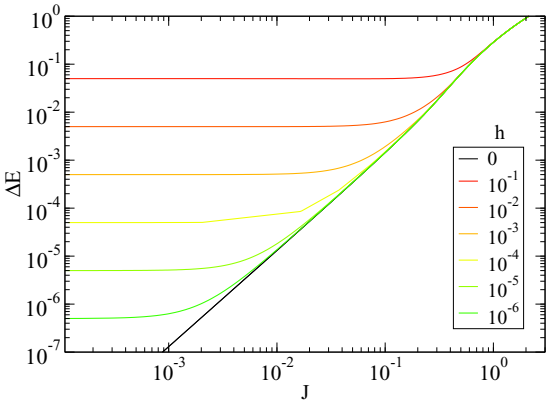

FIG. 7. Energy gain ΔE in the presence of the magnetic field. Here we use a flat band, and the chemical potential is fixed in the center of the band.

ACKNOWLEDGMENTS

The authors acknowledge the support of the Slovenian Research Agency (ARRS) under Grants No. P1-0044 and No. J1-7259 and thank J. Mravlje for comments.

APPENDIX A: MAGNETIC FIELD EFFECTS

We now briefly consider the energy gain of the impurity in the presence of the Zeeman term in the Hamiltonian:

$$H_{\mathrm{Zeeman}} = g_{\mathrm{imp}}\mu_B B S_z + \sum_k g_{\mathrm{bulk}}\mu_B B s_{z,k}. \tag{A1}$$

We take $g \equiv g_{\mathrm{imp}} = g_{\mathrm{bulk}}$ and express the field in units of the Zeeman energy, $h = g\mu_B B$. The results, displayed in Fig. 7, show the expected result: for small J the energy gain saturates at the value $\Delta E = h/2$ with the crossover occurring for J such that $\Delta E \approx h/2$. The value of T_K does not play any role here.

APPENDIX B: ANISOTROPIC KONDO COUPLING

The XXZ anisotropic Kondo model takes the following form:

$$H_{\mathrm{XXZ}} = J_\parallel S_z s_z + J_\perp(S_x s_x + S_y s_y). \tag{B1}$$

The extreme case is that of Ising-like coupling, $J_\perp \equiv 0$. There is no impurity dynamics in this limit, and the Hamiltonian becomes quadratic and hence exactly diagonalizable (see Appendix C). In the small-J and high-J limits, the energy gain for Ising coupling with $J_\parallel = J$ is one third of that in the regular isotropic Kondo model with Heisenberg coupling $J_\parallel = J_\perp = J$, while the nontrivial deviations due to many-particle physics occur in the intermediate-J range (see Fig. 8). The energy gain is always larger in the isotropic model even after accounting for the overall factor of 3. In the small-J asymptotic regime where $\Delta E_{\mathrm{Heisenberg}} \approx 3 \times \Delta E_{\mathrm{Ising}}$ to a good approximation, the Kondo temperature is smaller than ΔE already by many orders of the magnitude.

We have also computed the difference of the energy gain for isotropic exchange and three times the energy gain for Ising coupling. The result is plotted in the inset in Fig. 8 in the form of the logarithmic derivative of the quantity. Considering that

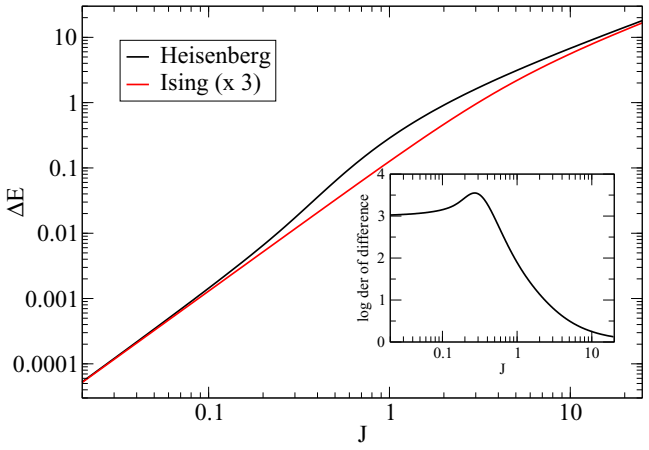

FIG. 8. Energy gain ΔE in the anisotropic Kondo model with exchange coupling of Ising type, $J_\parallel = J$ and $J_\perp = 0$, and in the isotropic model with exchange coupling of Heisenberg type, $J_\parallel = J_\perp = J$. The result for the Ising coupling is multiplied by 3 for easier comparison. We use a flat band with μ fixed in its center. The inset shows the logarithmic derivative of $(\Delta E)_{\text{Heisenberg}} - 3(\Delta E)_{\text{Ising}}$, thus indicating the power-law exponent of the correction due to spin-flip dynamics.

the quadratic term in the energy gain is entirely due to the spin-dependent scattering on a static local moment, we see that the leading contribution to the ground-state energy of the spin-flip processes leading to the Kondo effect is of the order of J^3 (and not T_K).

APPENDIX C: ENERGY GAIN IN THE $J \to 0$ LIMIT

The energy gain in the small-J limit will now be calculated analytically. The calculation is performed using the equations of motion for a static impurity in the bulk:

$$H_{\text{kin}} = \sum_{k\sigma} \epsilon_k c^\dagger_{k\sigma} c_{k\sigma},$$
$$H_{\text{int}} = (2h) s_z(\mathbf{r} = 0). \tag{C1}$$

The factor 2 in $(2h)$ is included for convenience. For an $S = 1/2$ impurity, $h = J/4$. We now drop the spin index σ and focus on the $\sigma = \uparrow$ case; the sums over spin are performed by taking $h \to -h$ for $\sigma = \downarrow$. The energy gain is defined as

$$\Delta E = \langle H \rangle_{J=0} - \langle H \rangle_J \tag{C2}$$

and can be split into two contributions:

$$\Delta E = (\Delta E)_{\text{kin}} + (\Delta E)_{\text{int}}. \tag{C3}$$

For the impurity T matrix we find

$$T(z) = \frac{1}{N}[h + h^2 \langle\langle f; f^\dagger \rangle\rangle_z], \tag{C4}$$

where N is the number of lattice sites in the system and $f = (1/\sqrt{N}) \sum_k c_k$, so that the k-resolved Green's function is

$$G_{kk'}(z) = G^0_k(z)\delta_{kk'} + G^0_k(z) \frac{1}{N}[h + h^2 \langle\langle f; f^\dagger \rangle\rangle_z] G^0_{k'}(z), \tag{C5}$$

with $G^0_k(z) = (z - \epsilon_k)^{-1}$ being the nonperturbed bulk Green's function. We note that

$$G_f(z) \equiv \langle\langle f; f^\dagger \rangle\rangle_z = \frac{1}{N} \sum_{kk'} G_{kk'}(z); \tag{C6}$$

hence we sum over k and k' to obtain

$$G_f(z) = G^0_{\text{loc}}(z) + G^0_{\text{loc}}(z)[h + h^2 G_f(z)] G^0_{\text{loc}}(z). \tag{C7}$$

The solution is

$$G_f(z) = \frac{G^0_{\text{loc}}(z)}{1 - h G^0_{\text{loc}}(z)}. \tag{C8}$$

For a flat band with half bandwidth D, the exact expression for $G^0_{\text{loc}}(z)$ is

$$G^0_{\text{loc}}(z) = -\frac{1}{2D} \ln \frac{z - D}{z + D}. \tag{C9}$$

We now calculate the energy gain due to the interaction term, $(\Delta E)_{\text{int}} = -\langle H_{\text{int}} \rangle = -h(n_{f\uparrow} - n_{f\downarrow})$, with

$$n_{f\sigma} = \langle f^\dagger_\sigma f_\sigma \rangle = \int_{-\infty}^{\infty} f(\omega) d\omega \, \frac{-1}{\pi} \text{Im} G_{f\sigma}(z), \tag{C10}$$

with $f(\omega)$ being the Fermi function. We take the difference

$$h[G_{f\uparrow}(z) + (h \to -h)] = \frac{2h^2 G^0_{\text{loc}}(z)}{1 - h^2 \left[G^0_{\text{loc}}(z)\right]^2} \approx 2h^2 \left[G^0_{\text{loc}}(z)\right]^2. \tag{C11}$$

Then

$$(\Delta E)_{\text{int}} = \frac{2h^2}{\pi} \int_{-\infty}^{\infty} \text{Im}\left\{\left[G^0_{\text{loc}}(\omega + i\delta)\right]^2\right\} f(\omega) \, d\omega. \tag{C12}$$

Noting that, for $z = \omega + i\delta$,

$$\text{Im}\left[G^0_{\text{loc}}(z)\right]^2 = 2\text{Im}G^0_{\text{loc}}(z)\text{Re}G^0_{\text{loc}}(z) = 2\pi\rho^2 \ln \frac{D - \omega}{D + \omega} \tag{C13}$$

and integrating over ω at $T = 0$, we finally find

$$(\Delta E)_{\text{int}} = 8 \ln 2 (\rho h)^2 D = \frac{\ln 2}{8} (J/D)^2 D. \tag{C14}$$

The total energy gain can now be computed using the formula

$$\Delta E = \int_0^J \frac{dJ'}{J'} \langle H_1 \rangle_{J'}, \tag{C15}$$

where the expectation value is that of the interaction part of the Hamiltonian, here equal to $(\Delta E)_{\text{int}}$ evaluated at $J = J'$ [see also Eq. (11) with $\beta = 2$]. Alternatively, we can explicitly calculate the band contribution $(\Delta E)_{\text{bulk}}$. The kinetic energy is

$$E_{\text{kin}} = \sum_k \epsilon_k n_k, \tag{C16}$$

with

$$n_k = \int_{-\infty}^{\infty} A_k(\omega) f(\omega) d\omega \tag{C17}$$

and

$$A_k(\omega) = -\frac{1}{\pi}\mathrm{Im}G_{kk}(\omega + i\delta). \tag{C18}$$

The first term in G_{kk} cancels out after subtracting the energy of the system without the impurity. Thus

$$(\Delta E)_{\mathrm{kin},\sigma} = \frac{1}{\pi}\sum_k \epsilon_k \int_{-\infty}^{\infty} d\omega \times \mathrm{Im}\left\{\frac{1}{z-\epsilon_k}\frac{1}{N}[h + h^2 G_f(z)]\frac{1}{z-\epsilon_k}\right\} f(\omega). \tag{C19}$$

This has to be summed over spin. Recalling that h changes sign, the first term cancels out, and

$$h^2[G_f(z) + (h \to -h)] = 2h^2 \frac{G^0_{\mathrm{loc}}(z)}{1 - h^2\left[G^0_{\mathrm{loc}}(z)\right]^2} \approx 2h^2 G^0_{\mathrm{loc}}(z). \tag{C20}$$

For small h we are left with ($z = \omega + i\delta$)

$$\Delta E_1 = 2\frac{h^2}{\pi}\frac{1}{N}\sum_k \epsilon_k \int_{-\infty}^{\infty} d\omega\, \mathrm{Im}\left(\frac{1}{z-\epsilon_k} G^0_{\mathrm{loc}}(z) \frac{1}{z-\epsilon_k}\right) f(\omega) = 2\frac{h^2}{\pi}\int \epsilon\rho(\epsilon)d\epsilon \int_{-\infty}^{\infty} d\omega\, \mathrm{Im}\left(\frac{1}{z-\epsilon} G^0_{\mathrm{loc}}(z) \frac{1}{z-\epsilon}\right) f(\omega). \tag{C21}$$

The ϵ integral can be evaluated for a flat band (using $D = 1$):

$$\int_{-1}^{1} \frac{\epsilon}{(z-\epsilon)^2} d\epsilon = \frac{2z}{z^2-1} + \ln\frac{z-1}{z+1} \equiv F(z). \tag{C22}$$

Then at $T = 0$

$$(\Delta E)_{\mathrm{kin}} = -\frac{2(h\rho)^2}{\pi}\mathrm{Im}\left[\int_{-\infty}^{0} F(\omega + i\delta) g(\omega + i\delta) d\omega\right], \tag{C23}$$

where $g(z) = -\ln\frac{z-D}{z+D}$. The integration gives $2\pi \ln 2$. Thus

$$(\Delta E)_{\mathrm{kin}} = -\frac{\ln 2}{16}(J/D)^2 D. \tag{C24}$$

We finally obtain

$$\Delta E = \frac{\ln 2}{16}(J/D)^2 D. \tag{C25}$$

This agrees within a few per mill with the numerical renormalization-group results for the gain in the ground-state energy in the small-J limit of an Ising-coupled magnetic impurity. For a full isotropic coupling, we find exactly three times as much:

$$\Delta E = \frac{3\ln 2}{16}(J/D)^2 D, \tag{C26}$$

again in full agreement with the numerical calculation. The leading correction due to dynamic processes is $O(J^3)$, as demonstrated in Appendix B.

[1] Y. E. Shchadilova, M. Vojta, and M. Haque, Single-impurity Kondo physics at extreme particle-hole asymmetry, Phys. Rev. B **89**, 104102 (2014).

[2] A. C. Hewson, *The Kondo Problem to Heavy Fermions* (Cambridge University Press, Cambridge, 1993).

[3] K. G. Wilson, The renormalization group: Critical phenomena and the Kondo problem, Rev. Mod. Phys. **47**, 773 (1975).

[4] H. R. Krishna-murthy, J. W. Wilkins, and K. G. Wilson, Renormalization-group approach to the Anderson model of dilute magnetic alloys. I. Static properties for the symmetric case, Phys. Rev. B **21**, 1003 (1980).

[5] R. Bulla, T. Costi, and T. Pruschke, The numerical renormalization group method for quantum impurity systems, Rev. Mod. Phys. **80**, 395 (2008).

[6] R. Žitko and T. Pruschke, Energy resolution and discretization artifacts in the numerical renormalization group, Phys. Rev. B **79**, 085106 (2009).

[7] R. Žitko, Adaptive logarithmic discretization for numerical renormalization group methods, Comput. Phys. Commun. **180**, 1271 (2009).

[8] R. Žitko, J. Bonča, and T. Pruschke, Van Hove singularities in the paramagnetic phase of the Hubbard model: A DMFT study, Phys. Rev. B **80**, 245112 (2009).

[9] R. Žitko, Numerical renormalization group calculations of ground-state energy: Application to correlation effects in the adsorption of magnetic impurities on metal surfaces, Phys. Rev. B **79**, 233105 (2009).

[10] J. Kondo, Ground-state energy shift due to the *s-d* interaction, Phys. Rev. **154**, 644 (1967).

[11] A. K Mitchell, M. Vojta, R. Bulla, and L. Fritz, Quantum phase transitions and thermodynamics of the power-law Kondo model, Phys. Rev. B **88**, 195119 (2013).

[12] O. Ujsaghy, K. Vladar, G. Zaránd, and A. Zawadowski, The role of electron-hole symmetry breaking in the kondo problems, J. Low Temp. Phys. **126**, 1221 (2002).